Gold-sputtered microelectrodes with built-in gold reference and counter electrodes for electrochemical DNA detection

ARTICLE

Gold-sputtered microelectrodes with built-in gold reference and counter electrodes for electrochemical DNA detection

Received 00th January 20xx,
Accepted 00th January 20xx

DOI: 10.1039/x0xx00000x

Saranya Thiruvottriyur Shanmugam [a, b], Stanislav Trashin [a, b], Karolien De Wael [a, b*]

Gold-sputtered microelectrodes with built-in gold reference and counter electrodes represent a promising platform for the development of disposable DNA sensors. Pretreating gold electrode surfaces and immobilization of DNA thereon is commonly employed in biosensing applications. However, with no scientific or practical guidelines to prepare a DNA sensor using these miniature gold-sputtered microelectrodes, cleaning and immobilization steps need to be systematically optimized and updated. In this work, we present efficient cleaning and modification of miniaturized gold-sputtered microelectrodes with thiolated DNA probes for DNA detection. Additional discussions on subtleties and nuances involved at each stage of pretreating and modifying gold-sputtered microelectrodes are included to present a robust, well-founded protocol. It was evident that the insights on cleaning polycrystalline gold disk electrodes with a benchmark electrode surface for DNA sensors, cannot be transferred to clean these miniature gold-sputtered microelectrodes. Therefore, a comparison between five different cleaning protocols was made to find the optimal one for gold-sputtered microelectrodes. Additionally, two principally different immobilization techniques for gold-sputtered microelectrode modification with thiolated ssDNA were compared i.e., immobilization through passive chemisorption and potential perturbation were compared in terms of thiol-specific attachment and thiol-unspecific adsorption through nitrogenous bases. The hybridization performance of these prepared electrodes was characterized by their sensitive complementary DNA capturing ability, detected by a standard alkaline phosphatase assay. Immobilization through passive chemisorption proved to be efficient in capturing the complementary target DNA with a detection limit of 0.14 nM and sensitivity of 9.38 A M^{-1} cm^2. In general, this work presents a comprehensive understanding of cleaning, modification and performance of gold-sputtered microelectrodes with built-in gold reference and counter electrodes for both fundamental investigations and practical DNA sensing applications.

Introduction

The need for miniaturization in the field of electrochemical biosensors demands reproducible, cost-efficient and easy-to-use transducers with well-controlled properties. Generally, conventional polycrystalline gold disk electrodes are often used to demonstrate new detection principles in the development of biosensors. These electrodes are not intended to be single-use and must be pretreated carefully before each use, which is time-consuming. Disposable gold screen printed electrodes are already available on the market as an alternative to the conventional electrodes. More recently, gold-sputtered microelectrodes have become commercially available as an attractive platform for the development of miniaturized biosensors through covalent attachment of biomolecules to the gold surface via thiols [1-5]. These microelectrodes are made up of gold, sputtered with a thickness of 10–500 nm on a glass substrate directly or through an intermediate layer of chromium for better adhesion [1]. A single unit includes working, reference and counter electrodes, all made of sputtered gold, to operate in a small drop of liquid. In contrast to gold screen-printed electrodes made with conducting inks of complex composition, gold-sputtered microelectrodes are made of pure gold and, thus, resemble conventional polycrystalline gold electrodes. The latter are polished and pretreated chemically and/or electrochemically before use [6], whereas, gold-sputtered microelectrodes cannot be subjected to polishing but can be washed and pretreated chemically and/or electrochemically.

In general, chemical pretreatment of gold surfaces in piranha solution leads to severely oxidized gold, while aqua regia etches the gold contaminating the surface with chloride and does not result in significantly cleaner surfaces [7]. Electrochemical methods, especially, reductive potential sweep in alkaline solutions and oxidative potentials in acidic solutions, have proven to be effective for removing surface contaminants [8]. After chemical and/ or electrochemical pretreatment, gold surfaces can be modified by a bio-recognition element such as an ssDNA-probe or an oligonucleotide functionalized by a thiol at one of its ends.

[a] AXES Research Group, Department of Bioengineering, University of Antwerp, Groenenborgerlaan 171, 2020 Antwerp, Belgium.
[b] NANOlab Center of Excellence, University of Antwerp, Groenenborgerlaan 171, 2020 Antwerp, Belgium

Electronic Supplementary Information (ESI) available as a pdf file. See DOI:

Two principally different immobilization strategies exist for tethering DNA-probes through Au-S bonds. First, the electrode surface can be incubated in a solution of thiolated oligonucleotides in a high-ionic-strength buffer (usually for 16 – 24 h) followed by back-filling with mercaptohexanol (MH) or another functionalized short-chain thiol, which may also be added in the solution of the oligonucleotide for better control of oligonucleotide surface density [1, 9-13]. Second, taking advantage of the negatively charged backbone of DNA, the immobilization can be promoted by applying a sufficiently positive constant potential [3] or by quick switching of the potential to create microscale "stirring" or perturbation of the solution near the electrode surface due to migration of ions induced by charging/discharging of the double-layer capacitance [14-19]. Nevertheless, little information was reported on optimization of electrochemical pretreatment of gold-sputtered electrodes, their voltammetric characterization in sulphuric acid (to assess the cleanliness and roughness)[8, 20], comparison of immobilization strategies via thiols including control measurements with non-thiolated sequences. As per our knowledge, none of the literature reported these for gold-sputtered microelectrodes with in-situ gold reference and counter electrodes. This motivated us to study the preparation of such microelectrodes for biosensing applications given their asset of being able to offer high sensitivity, easy operation and portability.

In this article, we compare five cleaning protocols for gold-sputtered microelectrodes as it was evident that the insights on cleaning polycrystalline gold disk electrodes with a benchmark electrode surface for DNA sensors, cannot be transferred to clean these miniature gold-sputtered microelectrodes. Secondly, two strategies for immobilization of thiolated oligonucleotides (*i.e.*, attachment through the conventional chemisorption and the immobilization through potential perturbation) are tested. Special attention has been paid to a side-by-side comparison of thiol-specific attachment and weak unspecific adsorption of oligonucleotides. Finally, hybridization performance of this miniaturized DNA sensor has been checked using biotin-labelled complementary DNA strands. The detection is based on alkaline phosphatase (ALP) assay for enzymatic signal amplification, a well- known optical or electrochemical enzymatic assay used in the detection of DNA in other gold platforms [2, 21, 22].

Experimental

Equipment

Electrochemical pretreatment and characterization of electrodes were carried out using µAutolab III (Metrohm-Autolab BV). PalmSens3 (PalmSens BV) was used to detect hybridization. Gold-sputtered microelectrodes were purchased from Micrux Technologies (Oviedo, Spain). The diameter of the gold working electrode was 1 mm (Figure S6). The sample volume applicable to the sensor is in the range between 1 and 15 µL. We have used 5-10 µL for modification and in detection stages. The measurements were carried out with the electrode connector assembly (AIO Drop Cell-Base) from the same company. The external electrochemical setup, polycrystalline gold disk electrode (1.6 mm in diameter) was purchased from BASi, USA. Saturated calomel electrode (SCE, radiometer, Denmark) was used as an external reference electrode. The SCE was separated by a frit to avoid any contamination of the working solution with Cl^-. Scanning electron microscopy (SEM) images were taken by the FEI Quanta 250 (Thermo Fisher Scientific) at 30 kV.

Table 1 Pretreatment protocols for gold-sputtered microelectrodes.

Protocol	Sonication		Electrochemical pretreatment
	70% EtOH	MilliQ Water	Potential (V) -2.0 -1.0 0.0 1.0 2.0
1	✓	✓	
2*	✓	✓	2 V/s, 20 cycles 0.5 M NaOH; 0.1 V/s, 20 cycles 0.5 M H_2SO_4
3*	✓	✓	2 V/s, 20 cycles 0.5 M H_2SO_4; 0.1 V/s, 20 cycles 0.5 M H_2SO_4
4**	✓	✓	0.1 V/s, 12 cycles 0.05 M H_2SO_4
5**	✓	✓	0.1 V/s, 12 +12 cycles 0.5 M H_2SO_4
			-2.0 -1.0 0.0 1.0 2.0 Potential (V)

*performed in a three-electrode cell using an SCE as the reference electrode; **in a drop using pseudo-reference Au electrode. The arrow shapes depict cyclic voltammetry between the indicated potential window. Protocol 5 involves an initial 12 cycles of potential sweep after which the drop was refreshed and additional 12 cycles conducted. Protocol 2 is also used to electrochemically pretreat polycrystalline gold disk electrode after polishing.

Pretreatment of gold-sputtered microelectrodes

Gold-sputtered microelectrodes were pretreated using five different protocols (Table 1) that were adapted from the literature, inspired by the traditional methods for pretreating polycrystalline gold disk electrodes [3, 6, 20, 23, 24]. For comparison, polycrystalline gold disk electrodes were polished using alumina and diamond slurries (more information can be found in supplementary section) and electrochemically pretreated in NaOH and H_2SO_4 identically to protocol 2 for the gold-sputtered electrodes. To electrochemically characterise the working electrode surface after pretreatment procedures, cyclic voltammetry was carried out in 0.5 M H_2SO_4 using a separate three-electrode cell by connecting only the working electrode of the gold-sputtered microelectrodes and using external saturated calomel electrode as the reference and platinum rod as a counter electrode. The electrochemically available surface area was estimated from the cyclic voltammograms (CV) in 0.5

M H_2SO_4 [25] by taking the charge accumulated during the reduction of gold oxide to the reference value (400 $\mu C/cm^2$). Then, the surface roughness (R_f) was calculated as the ratio of electrochemically available and geometric surface area.

Modification reagents

Oligonucleotides were obtained from Eurogentec (Belgium). Their structures and purity were confirmed by mass spectrometry. The oligonucleotide sequence was chosen to be complementary to microRNA-21 (miR-21), a marker for several types of cancer and cardiovascular diseases [26]. Thiolated probe (complementary): HS-(CH2)6-5'TAG-CTT-ATC-AGA-CTG-ATG-TTG-A3'; non-thiolated probe (complementary): 5' TAG-CTT-ATC-AGA-CTG-ATG-TTG-A 3'; Thiolated probe (non-complementary): HS-(CH_2)6- 5' TAG-CTT-ATG-TGT-ACC-CTG-TCA-G 3'; Target: Biotin-5'-TEG-TCA-ACA-TCA-GTC-TGA-TAA-GCT-A 3'. Immobilization (Tris) buffer contained 500 mM KCl, 50 mM $MgCl_2$, and 10 mM tris pH 7.5. The washing (Tris-T_{20}) buffer had the same composition but additionally contained 0.05% w/v tween 20.

Immobilization of ssDNA through chemisorption

Initially, 20 µL solution containing 1 µM probe DNA with 0.1 mM tris (2-carboxyethyl) phosphine (TCEP) and 0.2 µM of either mercaptohexanol (MH) or mercaptobutanol (MB) or mercaptoundecanol (MU, in 30% ethanol) in immobilization buffer (Tris buffer) was dropped on the electrode surface and left for overnight incubation (~16 hours) at room temperature in a closed Petri dish with a wet paper inside to avoid evaporation of the droplet (Fig. S4). The electrodes were then transferred into vials containing Tris buffer and washed gently by replacing Tris buffer five times. This was followed by incubation for 2 hours in a 1 mM back-filling thiol in Tris buffer. Then electrodes were rinsed and stored in Tris buffer avoiding complete drying of the surface between these steps to ensure good reproducibility of the procedure.

Immobilization through potential perturbation

Experimental parameters for this method were adapted from the literature[15, 16]. Potential pulses were applied between +0.3 V and −0.2 V vs Au pseudo-reference electrode. The upper and lower potentials were determined from the available potential window limited by the reductive desorption thiols in the cathodic region and Au-S oxidation and gold oxide formation in the anodic region as measured with cyclic voltammetry in 10 mM PB, 450 mM K_2SO_4 (Fig. S2). For the immobilization, 15 µL of 1 µM of probe DNA in 10 mM PB, 450 mM K_2SO_4 was placed on the microelectrode's working area and perturbed for 2 minutes between +0.3 V and −0.2 V with 10 ms interval time. Then, the electrode was washed gently with a solution containing 10 mM PB and 450 mM K_2SO_4. Afterwards, 15 µL of 1 mM thiol (MH/ MB/MU) solution in 10 mM PB, 20 mM K_2SO_4 was placed on the electrode and perturbed for 1 min between +0.3 V and −0.2 V with 10 ms interval time. Finally, the electrodes were washed with buffer containing 10 mM PB, 20 mM K_2SO_4.

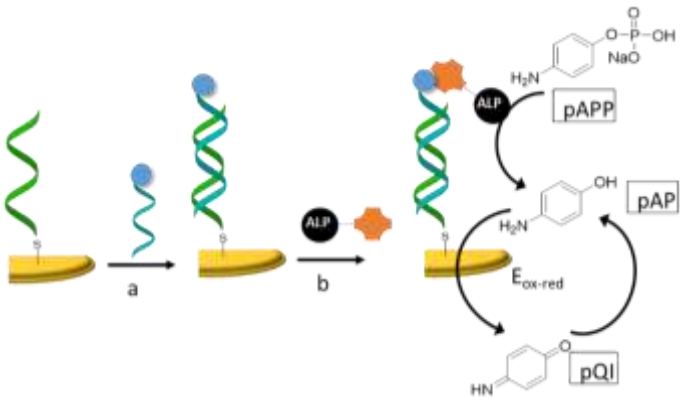

Figure 1- A schematic illustration of DNA hybridization with biotinylated target sequence (a) and detection strategy based on enzymatic assay (b). Alkaline phosphatase (ALP) tagged streptavidin binds to biotinylated target which hydrolyses pAPP into pAP which in turn gets oxidized at the electrode surface.

Estimation of probe density on the surface

The probe density was measured by chronocoulometry through adsorption of ruthenium (III) hexamine chloride (RuHex) in 10 mM tris buffer (pH = 7.4) as described before [13]. Briefly, the potential step from +150 mV to −450 mV vs SCE was applied and the charge as a function of time was measured for 1000 ms. For each electrode, the measurements were first conducted in the pure buffer and then in the presence of 3.5 µM RuHex.

Hybridization with target DNA and detection

Modified electrodes were incubated for 1 hour in a solution of the biotinylated target DNA in Tris buffer at room temperature. Then, the electrodes were washed in Tris-T_{20} buffer and incubated in Tris-T_{20} buffer containing 0.75 µg/mL S-ALP for 20 minutes. The electrodes were then rinsed with Tris-T_{20} and stored in Tris buffer before the electrodes were characterized. Hybridized oligonucleotides were amperometrically detected due to formation of electroactive *p*-aminophenol (*p*AP) converted from *p*-aminophenyl phosphate (*p*APP) by streptavidin-alkaline phosphatase (ALP) conjugate [21] in a measuring buffer (50 mM Tris. HCl, 10 mM $MgCl_2$, pH 9.6) containing 3 mM pAPP (Fig. 1). The limit of detection (LOD) was calculated from the ratio of 3 times the standard deviation of the blank over the gradient of the calibration curve. While sensitivity was calculated from the ratio of the gradient of the calibration curve over the surface area. The Au built-in reference electrode of the prepared sensors showed adequate stability in the measuring buffer for at least first 10 min with an average potential of −0.056 ± 0.005 vs SCE (Figure S5). Amperometric readings for the calibration plot were made at 120 s.

Results and discussion

Pretreatment of gold-sputtered microelectrodes

The use of a well-controlled pretreatment protocol is critically important for the reproducible and efficient immobilization of biomolecules and SAM layers on gold surface [24]. Gold-sputtered microelectrodes cannot be mechanically polished and, thus, should be carefully cleaned chemically and/or electrochemically. Moreover, harsh chemical cleaning (e.g., by

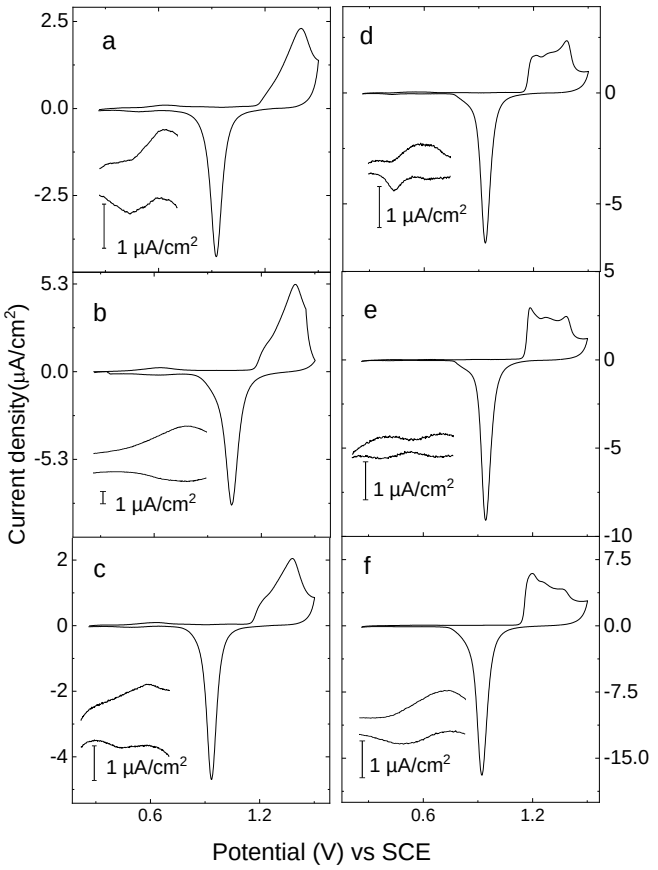

Figure 2 Cyclic voltammograms of gold-sputtered microelectrodes after pretreatment according to protocols 1—5 (a-e) in comparison to a polycrystalline gold disk electrode pretreated following protocol 2 after polishing with alumina and diamond micro particles (f). Measurements were carried out in 0.5 M H_2SO_4, with the SCE reference and platinum counter electrode. The insets zoom in the electrical double layer region of the respective voltammograms

piranha solution) is harmful to the chosen microelectrodes due to a thin layer of insulator around the working area. To test the cleanness of gold-sputtered microelectrodes and thus the quality of the five pretreatment protocols, we performed cyclic voltammetry in 0.5 M H_2SO_4 and compared the profiles with a well-established behaviour of pure polycrystalline gold electrodes [27].

The evaluation of the pretreatment quality was based on the shape of cyclic voltammograms (CV) in 0.5 M H_2SO_4 obtained in the same conditions for all electrodes using a conventional three-electrode cell with an SCE as the reference electrode. The working electrode's surfaces of the pretreated gold-sputtered microelectrodes were compared to mechanically polished and electrochemically pretreated polycrystalline gold disk electrodes (Fig. 2). The roughness (R_f) of the electrodes was calculated as the ratio of electrochemical and geometric surface area as described in the experimental section. R_f value of polished and pretreated polycrystalline gold disk electrodes was found to be 1.73 ± 0.05, whereas the apparent R_f values of planar gold electrodes varied with the pretreatment protocol.

Protocol 1 involves only cleaning with 70% ethanol and ultrapure water in an ultrasonic bath without any followed electrochemical pretreatment step. In comparison to the polycrystalline gold disk electrode (Fig. 2f), the CV after protocol 1 (Fig. 2a) showed near-complete suppression of the first peak at +1.16 V in the region of gold oxide formation. This suggests surface contamination [28] that remains after washing, partially blocking the gold surface. Thus, the calculated R_f value of 1.15 ± 0.04 is likely underestimated in these conditions, motivating, in general, the addition of an electrochemical step in the pretreatment. Protocol 2 introduces two electrochemical pretreatment steps (cathodic in 0.5 M NaOH and anodic in 0.5 M H_2SO_4) and exactly repeats the pretreatment protocol of the polycrystalline gold disk electrodes traditionally mechanically polished first. Surprisingly, the protocol was not efficient for the used gold-sputtered electrodes and resulted in an only minor difference in the shape of CV compared to the electrodes only washed in 70% ethanol (protocol 1). Nevertheless, R_f value slightly increased to 1.34 ± 0.04, which indicates better surface decontamination and motivates to further optimize the electrochemical pretreatment step.

The producer of the used gold-sputtered electrodes generally recommends cathodic and anodic electrochemical pretreatment both in H_2SO_4 in a wide potential window. Additionally, the use of only H_2SO_4 for both anodic and cathodic regions makes the protocol to be simpler and faster. Thus, we designed protocols 3 – 5 for further evaluation. Protocol 3 mimics protocol 2 but the cathodic electrochemical pretreatment was performed in 0.5 M H_2SO_4 instead of 0.5 M NaOH. This does not yield any considerable change in the shape of CV and R_f value (1.29 ± 0.12). In contrast, protocols 4 and 5 – based on the pretreatment in H_2SO_4 but in a wider potential window – were more successful. protocol 4 was applied in a drop of 0.05 M H_2SO_4. Though this caused some drift in the potential of the built-in pseudo-reference gold electrode, a stable cyclic voltammogram was observed by the end of the pretreatment step. However, the exposure to extreme anodic current density during such pretreatment resulted in damage and near-complete dissolution of the counter gold electrode. Nevertheless, the working electrode stayed undamaged, and a CV could be obtained in the three-electrode cell for comparison among the other protocols. The found R_f value of 1.36 ± 0.02 was rather the same as in protocol 2 and 3 but CV, in contrast, revealed the distinct gold oxide formation profile starting from +1.16 V (Fig. 2d) and a lower background current in the electrical double layer region indicating improved decontamination of the surface. The conditions were further modified to preserve the cleaning efficiency but avoid the physical damage of the counter electrode.

In protocol 5, the electrode was pretreated in a drop of 0.5 M H_2SO_4 but within a narrower potential window (between −1.0 V and +1.3 V instead of −1.5 and +1.5 V used in protocol 4). CV

shows the characteristic profile of gold oxide formation similar to the profile at the polycrystalline gold disk electrodes with three distinct peaks with the intense first peak at + 1.16 V. Moreover, the lowest currents in the double-layer region were observed suggesting efficient cleaning of the gold surface. In contrast, the R_f value of 1.76 ± 0.04 was calculated from CV

Table 2 Surface adsorption of RuHex on modified electrodes.

Immobilization method for ssDNA	Back-filling thiol[b]	$Ru(NH_3)_6^{3+}$ (pmol/cm²)[a]		
		SH-Oligo	Oligo	Blank control
Chemisorption	MB	87.4 ± 6.9	25.2 ± 1.4	13.2 ± 3.0
	MH	78.6 ± 3.5	21.1 ± 2.2	13.6 ± 1.0
	MU	55.3 ± 5.3	15.1 ± 2.1	7.5 ± 1.5
Potential perturbation	MB	30.4 ± 0.7	15.4 ± 0.6	11.3 ± 1.6
	MH	32.7 ± 1.3	24.0 ± 0.6	19.5 ± 1.6
	MU	17.3 ± 2.2	9.7 ± 0.8	6.9 ± 2.3

[a] Each value is depicted as an average ± standard error for at least three independent electrodes. [b] MB: mercaptobutanol, MH: mercaptohexanol, MU: mercaptoundecanol. SH-Oligo: thiolated probe, Oligo: non-thiolated probe.

after pretreatment by protocol 5 suggesting that the pretreated electrodes are rougher after protocol 5 than after protocols 1–4. Nevertheless, scanning electron microscopy (SEM) showed no noticeable topological difference between working electrodes pretreated according to protocol 1 (only sonication in 70% ethanol) and protocol 5 (Fig. S1). This confirms that the protocol 5 alters only a superficial layer of gold without its deep damage or partial dissolution, while, within Protocols 1–4, contamination may remain and cover a fraction of gold atoms on the surface resulting in apparently low roughness coefficient R_f. Thus, protocol 5 appeared to be the most promising for the electrode pretreatment and was chosen for the following work. Protocol 5 can also be used to recover electrodes after their chemical modification. Overnight incubation of the electrodes with the thiolated probe and MH solution resulted in the suppression of the first peak of gold oxide formation (at +1.16 V) and an increase of current in the electrical double layer region on CV in the same manner as it was observed for the electrodes pretreated according to protocols 1–3 (Fig. 2a-c, Fig. S3). However, after pretreatment according to protocol 5, the shape was completely recovered to that before modification.

Thiol-tethered immobilization of DNA probes

We compared conventional overnight chemisorption and immobilization through potential perturbation of DNA probes on the pretreated planar gold-sputtered electrodes. Surface density (coverage) of the ssDNA probe on the electrodes was measured by chronocoloulometry using RuHex, a multivalent redox cation interacting with the DNA backbone. A non-thiolated ssDNA probe of the same sequence was used as a control for assessment of non-specific adsorption of the oligonucleotide on the surface via weak interactions. Such adsorption is unwanted in general because it may reduce the hybridization efficacy due to the steric factor and poor probe spatial orientation [29]. Blank measurements without any DNA sequences (but only with back-filling thiols) served as blank controls. The amount of surface-confined RuHex was converted to apparent ssDNA surface coverages.

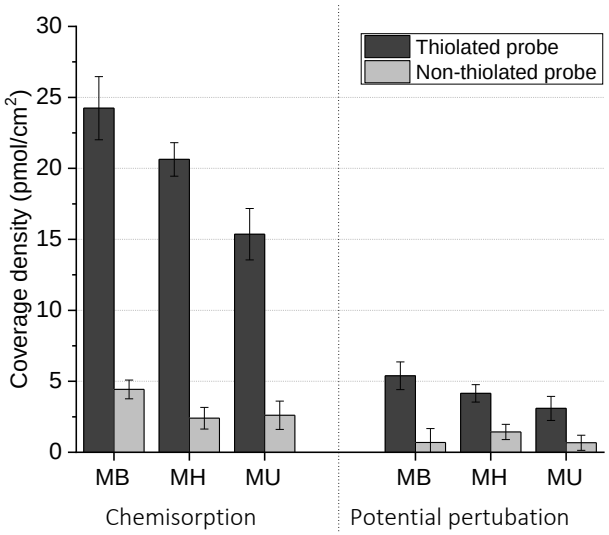

Figure 3 Comparison of coverage density of thiolated and non-thiolated probes between two immobilization methods. Error bars indicate the standard error of measurements with three independent electrodes

Table 2 lists the surface adsorption of RuHex for a series of electrodes prepared by two different strategies and using three back-filling thiols that differ by the carbon chain length. After correction of the values to the blank controls (Fig. 3), the probe surface coverages are in the range of 15–24 pmol/cm² (20.7 ± 1.2 for MH) for overnight chemisorption and 3–6 pmol/cm² (4.2 ± 0.6 for MH) for the potential perturbation method depending on the back-filling thiol. The probe coverage values from the potential perturbation method are rather in the low range of the values obtained in other studies [16, 30] and about 2–3 times lower compared to the coverage obtained in the optimized conditions for this method [16], which suggests that our conditions might be not optimal. Nevertheless, the overall coverage of the thiolated probe was 4–5 times higher for the overnight chemisorption in comparison to the potential perturbation method in our work and about 2 times higher compared to the reported maximal coverage for the potential perturbation method in optimized conditions [16]. Based on the theoretical calculations with a maximally dense arrangement of ssDNA, the expected surface coverage for a tightly packed ssDNA layer with a probe length of 22 bases should range between 25 and 30 pmol/cm² [12]. Thus, we estimate that around 80% of the maximal coverage was attained with overnight chemisorption and 20% with immobilization through the potential perturbation method. It is known that adsorption of oligonucleotides can occur on gold surfaces through non-covalent interactions of gold atoms and nitrogenous bases and may exceed 30% of the maximal probe coverage depending on the probe sequence and its length [11]. Nevertheless, in here, non-specific adsorption counted up to 14 ± 2% (2.4 – 3.8

pmol/cm^2) of the coverage for the thiolated probe in the procedure with chemisorbed ssDNA and 27 ± 6% (0.9 – 1.4 pmol/cm^2) for the potential perturbation method.

The chain length of the back-filling agents noticeably influenced the coverage in both procedures (Fig. 3). The highest coverage was obtained for mercaptobutanol (MB) and the lowest (by 40% compared to MB) coverage was obtained for mercaptoundecanol (MU). MU also resulted in lower blanks and lower coverage for thiol-unspecific adsorption which, however, was not considerably different from those obtained for mercaptohexanol (MH). Moreover, a drop of the MU solution spreads over all the surface of the microelectrode due to MU acting as a surfactant, which makes it practically difficult to handle. It was also reported that MH forms more stable layer compared to MB [31]. Thus, MH was selected for the following experiments as the back-filling agent in both procedures.

Hybridization efficiency at gold-sputtered microelectrodes

A higher surface coverage for an ssDNA probe does not necessarily guarantee higher responses to complementary DNA because the hybridization efficiency can be lowered by steric crowding effects for densely packed probes [29]. The overnight chemisorption provided approximately five times higher coverage of the probe compared to the immobilization through potential perturbation, but the latter should give more controlled and better-oriented assembly of the ssDNA probe due to the microscale stirring of the solution near the electrode [15, 30]. Here we evaluated side-by-side the hybridization efficiency for both immobilization methods at gold-sputtered microelectrodes.

To evaluate the ability to capture a specific sequence, we used the complementary and non-complementary (with scrambled bases) thiolated probes that were attached to the surface by both immobilization methods using MH as the back-filling agent. To ensure the adequate choice of the potential for amperometric detection of the ALP activity in the drop, cyclic voltammetry was firstly recorded in a conventional three-electrode cell containing 3 mM pAPP in the measuring buffer pH 9.6 (Fig. 4). Noteworthy, the built-in reference electrode was slightly affected by the immobilization procedure leading to a difference of 0.04 V between the built-in Au reference electrodes of the sensors prepared through overnight immobilization and the potential perturbation method (Fig. S7). This difference was taken into account for the following amperometric measurements.

In contrast to the electrode with the non-complementary probe, the electrode with the complementary probe can capture the biotinylated complementary target and, thus, also ALP-streptavidin conjugate via the biotin. An intense current peak at +0.4 V (Fig. 4) is specific for the electrode with the complementary probe and, thus, the peak was attributed to ALP activity, i.e. the electrochemical oxidation of pAP formed from pAPP. The second peak at +0.74 V was observed for both electrodes and was attributed to the oxidation of unhydrolyzed pAPP. To avoid an increased background current, the amperometric detection was carried out at a constant potential of +0.45 V, which is sufficient to detect the pAP formation but to avoid the increased background. Because of a small difference in the built-in reference electrodes as mentioned above, the peak was slightly shifted in case of the potential perturbation immobilization method. To compensate this, a potential of +0.50 V was applied to ensure the accurate comparison between the immobilization protocols.

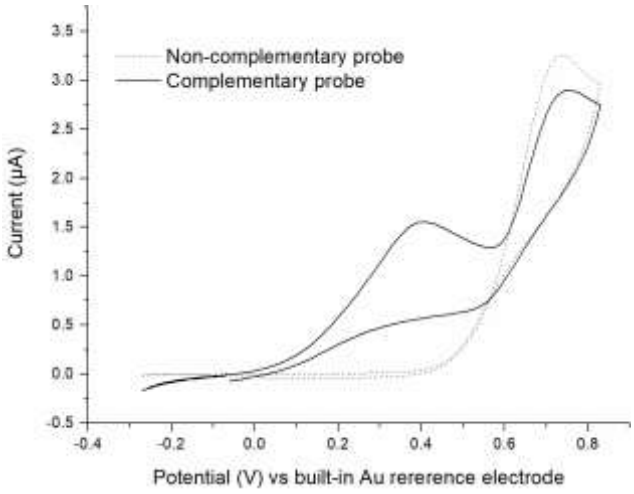

Figure 4 Cyclic voltammograms of the ssDNA modified (through chemisorption) electrodes after the DNA-detection step recorded in measuring buffer (50 mM Tris. HCl, 10 mM $MgCl_2$, pH 9.6) containing 3 mM pAPP. Scan rate, 0.1 V/s.

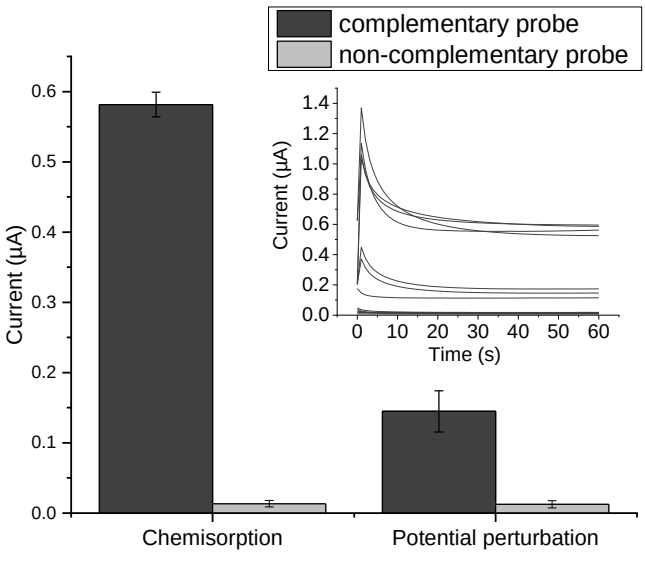

Figure 5. Amperometric responses ssDNA-modified electrodes after incubation in 20 nM target DNA labelled with biotin followed by treatment with the alkaline phosphatase-streptavidin conjugate. Potential applied, +0.45 V for chemisorption and +0.50 for potential perturbation (to compensate the difference between the potentials of the built-in Au reference electrodes). Error bars indicate the standard error from measurements with three independent electrodes. The inset shows the actual amperometric traces.

Both, conventional chemisorption and the potential-perturbation immobilization showed well-detectable responses to the target oligonucleotide (Fig. 5). The responses from the complementary probes exceeded 45 and 11 times the responses of the controls (scrambled sequences) for the overnight chemisorption and the potential perturbation

immobilization, respectively. The electrodes with a more densely packed probe obtained via overnight chemisorption resulted in four times higher average response compared to the electrode modified by the potential pulse assisted method. This difference is close to the ratio in the amount of immobilized ssDNA (4.9 ± 1.3 times). From this, we conclude

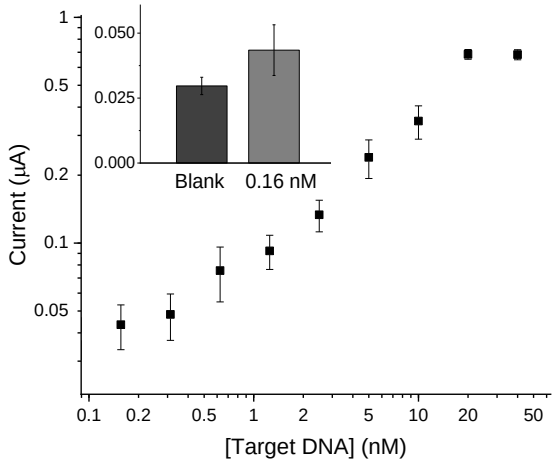

Figure 6 Calibration plot for Target-DNA detection from electrodes prepared through conventional chemisorption.

that the hybridization efficiency was not altered noticeably by the higher density of the probes. Thus, we evaluated the response of the sensors prepared through overnight chemisorption in the detection of different amounts of target DNA. Calibration curve from this experiment resulted in LOD of 0.14 nM and a sensitivity of 9.38 A M^{-1} cm^{-2} (Fig. 6).

It is noteworthy that the use of unoptimized cleaning protocols 1 and 2 lowered responses of the sensor to the complementary sequence and increased unspecific responses measured with the scrambled non-complementary probe (Table S1). The amplitude of the response was only 21% after protocol 1 and 49% after protocol 2 compared to protocol 5. The non-specific response was also 4 times higher for both protocol 1 and 2 compared to protocol 5. This shows the superiority of protocol 5 and motivates introducing an electrochemical cleaning step in addition to mechanical cleaning in an ultrasonic bath that rather removes large dust particles.

Taking into account the need of a potentiostat and one-by-one handling during the potential perturbation method, the overnight chemisorption is advantageous in its simplicity, higher throughput and eventually increased sensitivity in DNA sensing at gold-sputtered microelectrodes. Nevertheless, the potential perturbation method can provide reproducible ssDNA immobilization and thiol back-filling within minutes (about 30 min in total for a set of 6 electrodes), which makes it attractive for systems which require a minimum density of probes but faster immobilization procedure.

Conclusions

Two critical steps in constructing electrochemical DNA sensors based on gold-sputtered microelectrodes with built-in gold reference and counter electrodes were optimized in this work: (1) electrochemical pretreatment of the gold working surface and (2) thiol mediated tethering of ssDNA probes on it, (3) followed by its detection capabilities. Cyclic potential sweep between −1.0 and +1.3 V in a drop of 0.5 M H_2SO_4 was found to be the most effective procedure to clean the gold-sputtered microelectrodes, thus, improving the ease of preparation of electrode surface, compared to the situation, when one has to address conventional polycrystalline gold disk electrodes. The freshly pretreated gold-sputtered microelectrodes were effectively modified by a thiolated ssDNA probe through overnight chemisorption in a high ionic strength buffer. This resulted in about 70% of the maximal theoretical surface coverage (similar to conventional polycrystalline gold disk electrodes) and efficient hybridization capability. The modified electrodes could detect a complementary oligo resulting in an intense amperometric response 45 times higher compared to non-complimentary blank control. To sum up, this work introduces an essential toolbox for surface preparation and modification and usage of commercial gold-sputtered microelectrodes as the cost-efficient platform for DNA sensors. These optimized protocols can be adapted to other sputtered gold working electrode surfaces (with printed/sputtered reference and counter electrodes made from gold or other elements) that are now emerging in the market as disposable gold electrode platforms.

Conflicts of interest

There are no conflicts to declare

Acknowledgements

The authors thank the University Research Fund (BOF-DOCPRO), University of Antwerp, for financial support. Also funding from FWO is acknowledged.

References

1. E. O. Blair and D. K. Corrigan, *Biosens Bioelectron*, 2019, **134**, 57-67.
2. D. Xu, K. Huang, Z. Liu, Y. Liu and L. Ma, *Electroanalysis*, 2001, **13**, 882-887.
3. Z. A. Carter and R. Kataky, *Sensors and Actuators B: Chemical*, 2017, **243**, 904-909.
4. M. Santos-Cancel, R. A. Lazenby and R. J. White, *ACS Sens*, 2018, **3**, 1203-1209.
5. A. Toldrà, M. D. Furones, C. K. O'Sullivan and M. Campàs, *Talanta*, 2020, **207**, 120308.
6. R. F. Carvalhal, R. Sanches Freire and L. T. Kubota, *Electroanalysis*, 2005, **17**, 1251-1259.
7. R. P. Frankenthal and D. E. Thompson, *Journal of The Electrochemical Society*, 1976, **123**, 799-804.

8. L. M. Fischer, M. Tenje, A. R. Heiskanen, N. Masuda, J. Castillo, A. Bentien, J. Émneus, M. H. Jakobsen and A. Boisen, *Microelectronic Engineering*, 2009, **86**, 1282-1285.
9. J. I. A. Rashid and N. A. Yusof, *Sensing and Bio-Sensing Research*, 2017, **16**, 19-31.
10. V. Pagliarini, D. Neagu, V. Scognamiglio, S. Pascale, G. Scordo, G. Volpe, E. Delibato, E. Pucci, A. Notargiacomo, M. Pea, D. Moscone and F. Arduini, *Electrocatalysis*, 2018, **10**, 288-294.
11. R. Lao, S. Song, H. Wu, L. Wang, Z. Zhang, L. He and C. Fan, *Analytical Chemistry*, 2005, **77**, 6475-6480.
12. A. B. Steel, R. L. Levicky, T. M. Herne and M. J. Tarlov, *Biophys J*, 2000, **79**, 975-981.
13. A. B. Steel, T. M. Herne and M. J. Tarlov, *Analytical Chemistry*, 1998, **70**, 4670-4677.
14. Z. L. Yu, C. W. Yang, E. Triffaux, T. Doneux, R. F. Turner and D. Bizzotto, *Anal Chem*, 2017, **89**, 886-894.
15. D. Jambrec, F. Conzuelo, B. Zhao and W. Schuhmann, *Electrochimica Acta*, 2018, **276**, 233-239.
16. D. Jambrec, Y. U. Kayran and W. Schuhmann, *Electroanalysis*, 2019, DOI: 10.1002/elan.201900233.
17. U. Rant, K. Arinaga, S. Scherer, E. Pringsheim, S. Fujita, N. Yokoyama, M. Tornow and G. Abstreiter, *Proceedings of the National Academy of Sciences*, 2007, **104**, 17364-17369.
18. U. Rant, K. Arinaga, S. Fujita, N. Yokoyama, G. Abstreiter and M. Tornow, *Nano Letters*, 2004, **4**, 2441-2445.
19. K. K. Leung, H.-Z. Yu and D. Bizzotto, *ACS Sensors*, 2019, **4**, 513-520.
20. X. Xu, A. Makaraviciute, J. Pettersson, S.-L. Zhang, L. Nyholm and Z. Zhang, *Sensors and Actuators B: Chemical*, 2019, **283**, 146-153.
21. M. Gębala, L. Stoica, D. Guschin, L. Stratmann, G. Hartwich and W. Schuhmann, *Electrochemistry Communications*, 2010, **12**, 684-688.
22. S. Ma, Y. Hu, Q. Zhang, Z. Guo, S. Wang, Q. Shen, C. Liu and Z. Liu, *Sensors and Actuators B: Chemical*, 2018, **273**, 760-770.
23. A. Makaraviciute, X. Xu, L. Nyholm and Z. Zhang, *ACS Appl Mater Interfaces*, 2017, **9**, 26610-26621.
24. Y. Xiao, R. Y. Lai and K. W. Plaxco, *Nature Protocols*, 2007, **2**, 2875.
25. M. Łukaszewski, *International Journal of Electrochemical Science*, 2016, DOI: 10.20964/2016.06.71, 4442-4469.
26. R. Tavallaie, S. R. De Almeida and J. J. Gooding, *Wiley Interdiscip Rev Nanomed Nanobiotechnol*, 2015, **7**, 580-592.
27. J. P. Hoare, *Journal of The Electrochemical Society*, 1984, **131**.
28. B. E. Conway, H. Angerstein-Kozlowska, W. B. A. Sharp and E. E. Criddle, *Analytical Chemistry*, 1973, **45**, 1331-1336.
29. F. Ricci, R. Y. Lai, A. J. Heeger, K. W. Plaxco and J. J. Sumner, *Langmuir*, 2007, **23**, 6827-6834.
30. D. Jambrec, M. Gebala, F. La Mantia and W. Schuhmann, *Angew Chem Int Ed Engl*, 2015, **54**, 15064-15068.
31. L. Srisombat, A. C. Jamison and T. R. Lee, *Colloids and Surfaces A: Physicochemical and Engineering Aspects*, 2011, **390**, 1-19.